J Electroceram (2008) 21:653–656
DOI 10.1007/s10832-007-9273-5

Effect of seed layers on dielectric properties of $Ba(Zr_{0.3}Ti_{0.7})O_3$ thin films

Cheng Gao · Jiwei Zhai · Xi Yao

Published online: 21 August 2007

Abstract The Barium zirconium titanate $Ba(Zr_{0.3}Ti_{0.7})O_3$ thin films were prepared on $Pt/Ti/SiO_2/Si$ substrates with seed layers at the BZT/Pt interface by sol–gel process. Microstructure and structure of thin films were examined. Dielectric properties of thin films with various seed layers thicknesses were investigated as a function of frequency and direct current electric field. The tunability and dielectric constant of BZT thin films increased with increasing seed layer thickness from 0 to 20 nm, while it decreased with a further increase in thickness above 20 nm, meanwhile, the leakage current showed the similar tendency at applied electric field of 250 kV/cm. The optimized seed layer thickness for BZT thin films plays an important role in maintaining the high tunability and low leakage current, which are suitable for microwave device applications.

Keywords BZT thin films · Dielectric properties · Seed layers

1 Introduction

Barium titanate is the most common ferroelectric oxide in the perovskite ABO_3 structure. Insulating $BaTiO_3$ is widely used as a capacitor because of its high dielectric constant. In order to increase the tunability of the dielectric constant under a biasing field and to reduce the dielectric loss tangent at low frequencies, Sr or Zr was used as an addition [1, 2]. The high dielectric constant value combined with low dissipation factor makes $(Ba_{1-x}Sr_x)TiO_3$ (BST) one of the promising candidates for dynamic random access memory (DRAM) applications. Recently, $Ba(Zr_xTi_{1-x})O_3$ has been chosen as an alternative to BST in the fabrication of capacitors because Zr^{4+} is chemically more stable than $Ti^{4+}$and has a larger ionic size to expand the perovskite lattice. [3–10]. Therefore, the conduction by electron hopping between Ti^{4+} and Ti^{3+}, if any, would be depressed by the substitution of Ti with Zr.

Various factors, such as the lattice mismatch and differences in thermal expansion between the film and the substrate, affect the microwave dielectric properties of thin films. It was reported that seed layers deposited between substrate and BST thin films could reduce the effects of these factors and the dielectric properties of BST thin films were improved. The effect of seed layers thickness on dielectric properties of BST thin films has also been studied [11]. But the effect of seed layers on BZT thin films was not studied up to the present.

In this study, seed layers having the same composition as the main layer $[Ba(Zr_{0.3}Ti_{0.7})O_3]$ were deposited on $Pt/Ti/SiO_2/Si$ substrates and annealed at 700 °C for 10 min each time. Improvements in dielectric properties were examined through the correlation between the microstructure and dielectric properties of the main BZT layers deposited on various thicknesses of seed layers.

2 Experimental

The calculated amount of barium acetate $[Ba(CH_3COO)_2]$, zirconium (IV) isopropoxide $[Zr(OC_3H_7)_4]$ and titanium (IV) isopropoxide $[Ti(OC_3H_7)_4]$ were used as raw materials to prepare BZT precursor sol. Acetic acid, ethylene glycol

C. Gao (✉) · J. Zhai · X. Yao
Function Materials Research Laboratory, Tongji University, Shanghai 200092, China
e-mail: gc781225@163.com

J. Zhai
e-mail: apzhai@mail.tongji.edu.cn

monoethyl ether and Acetylacetone were used as solvent and polymerizing agents, respectively. Barium acetate was heated and dissolved in acetic acid. After cooling to room temperature, $Zr(OC_3H_7)_4$ and $Ti(OC_3H_7)_4$ were added in this solution. The ethylene glycol monoethyl ether and Acetylacetone were added to control the viscosity and cracking of films and the solution was mixed and refluxed for 1 h. The concentration of the final solution was adjusted to 0.3 M. Then the hydrolyzed solution was aged for 24 h. $Ba(Zr0.3Ti0.7)O_3$ seed layers, at various thicknesses, were deposited on $Pt/Ti/SiO_2/Si$ substrates and then crystallized at 700 °C. The main BZT thin films were deposited on the seed layers by spin coating at 3,000 rpm for 20 s for each layer. The wet films were dried and annealed at 600 °C for 10 min. Finally thin films were crystallized at 700 °C for 30 min. The total thickness of 400 nm including seed layers was achieved by repeating the spin-coating-drying-annealing process.

The crystalline phase of the thin films was identified by X-ray diffraction (BRUKER D8 Advance diffractometer). The surface morphology of the films was studied using field-emission scanning electron microscopy (FEI Quanta 200 FEG). For the electrical measurements the top gold electrode 500 μm square was deposited by DC-sputtering. The current-voltage (I-V) characteristics were measured using a Keithley 6517A. The capacitance-voltage (C-V) and capacitance-frequency (C-f) were measured using an Agilent 4284A LCR meter.

3 Results and discussion

The X-ray diffraction patterns of the $Ba(Zr_{0.3}Ti_{0.7})O_3$ thin films with various seed layers thicknesses annealed at 700 °C are shown in Fig. 1. The X-ray patterns indicate that the samples are perovskite and polycrystalline structure irrespective of BZT seed layer thickness and can be characterized by the appearance of (100), (110), (200), (210) and (211) peaks in the XRD spectra. The polycrystalline nature in these thin films is due to a lattice mismatch between BZT thin film and the $Pt/Ti/SiO_2/Si$ substrates [12].

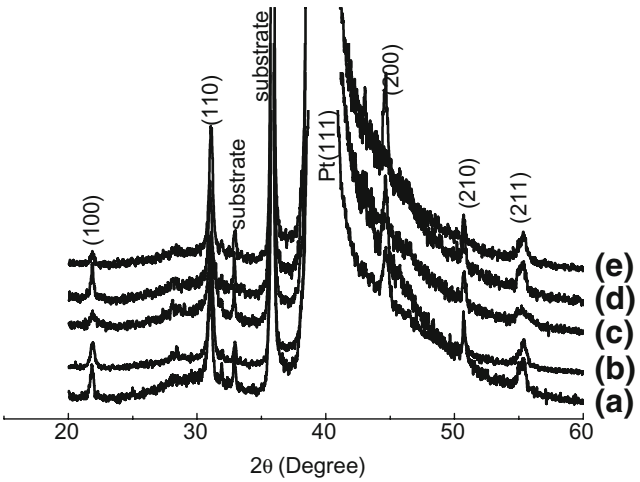

Fig. 1 X-ray diffraction patterns of BZT thin films with various seed layer thicknesses (*a*) 0 nm, (*b*) 10 nm, (*c*) 20 nm, (*d*) 40 nm, (*e*) 90 nm

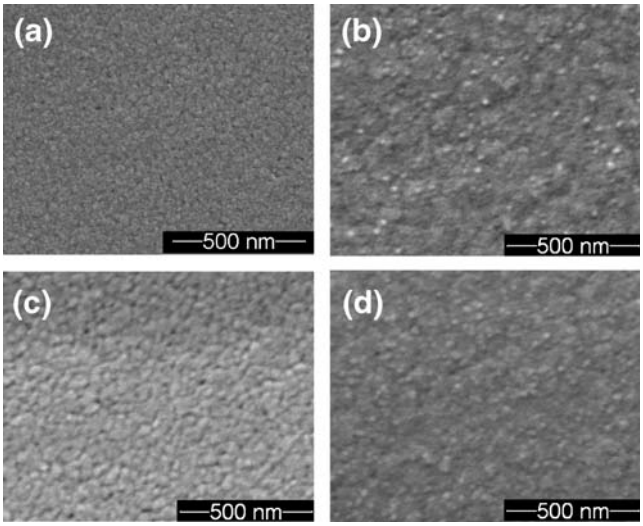

Fig. 2 Surface morphologies of BZT thin films deposited on seed layer of (**a**) 0 nm, (**b**) 10 nm, (**c**) 20 nm and (**d**) 90 nm in thickness

Figure 2 shows the surface morphological features of BZT thin films as revealed by the FESEM observations. The surface morphological features of the films appeared to be quite sensitive to the seed layer thickness. Through an analysis of these FESEM images, we have observed that BZT thin film with 20 nm seed layer in thickness reached a maximum in average grain size and became densest and smoothest in these thin films. The variation of grain morphologies was mainly controlled by the nucleation and growth rate, while the growth characteristics of BZT thin films deposited on seed layers below a 20-nm thickness was mainly influenced by Pt bottom electrode and the effect of seed layers gradually disappeared above 20-nm thickness because the BZT bulk characteristics appeared and increased above a critical thickness [11].

The dielectric properties of the BZT thin films in a Metal/Insulator/Metal (MIM) configuration were measured at room temperature as a function of the applied frequency and voltage. Figure 3 shows the evolution of the dielectric constant and loss tangent as a function frequency for the BZT films with various seed layer thickness. It can be seen that a slight decrease in dielectric constant with increasing frequency in the range of 1 kHz to 1 MHz. And above 200 kHz a rapid increase in the loss tangent can be observed. $Ba(Zr_{0.3}Ti_{0.7})O_3$ thin films is paraelectric at room temperature and do not possess any ferroelectric properties [13]. Therefore, spontaneous polarization cannot be generated at room temperature. Since there are no domain walls in these films, a ferroelectric dispersion cannot occur.

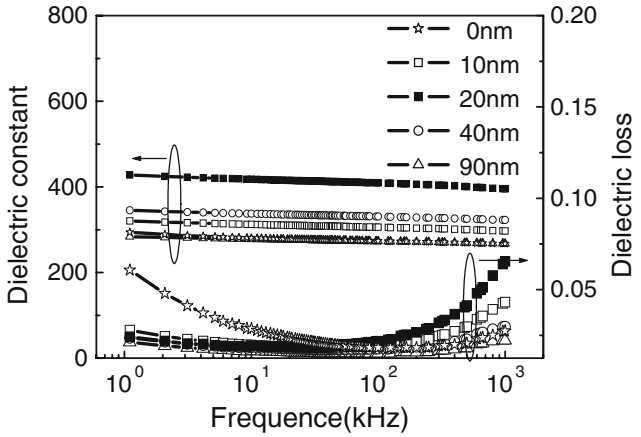

Fig. 3 Room temperature dielectric constant and dielectric loss of BZT thin films with different seed layer thickness as a function of the measuring frequency

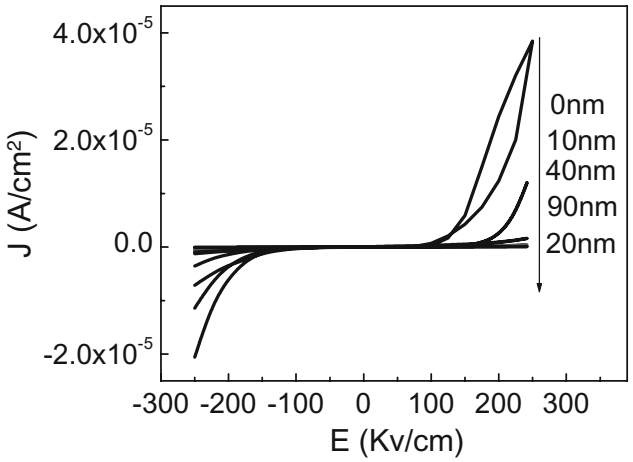

Fig. 5 The characteristics of the J–E curves for BZT thin films with different seed layer thickness obtained at room temperature

Therefore, a slight decrease in dielectric constant and increase in loss tangent at higher frequencies can be also observed. This behavior originates from the contact resistance and finite sheet resistance of both the bottom and top electrodes [14].

Dielectric constant and tunability as a function of seed layer thickness are given in Fig. 4. It can be seen that the value of the dielectric constant increased with increasing seed layer thickness up to 20 nm, while it decreased with a further increase in thickness above 20 nm at the measurement frequency of 100 kHz. The dielectric tunability showed the similar tendency at the frequency of 100 kHz and applied electric field of 250 kV/cm. In general, the tunability is roughly proportional to the dielectric constant. A material with higher dielectric constant possesses larger tunability [15]. The dielectric constant and tunability showed a maximum of 414 and 36.8%, respectively, at a seed layer thicknesses of 20 nm. This behavior is in good agreement with previous results by FESEM measurements that BZT thin film with 20-nm thickness seed layer reached a maximum in average grain size. Internal compressive stress occurs to a lesser extent in thin films with larger grains because of the lower concentration of grain boundaries and the direct effect of compressive stress may be the shift of the ionic positions in a unit cell and this causes the change in polarization, while the compressive stress decreases the dielectric constant of thin films [16, 17].

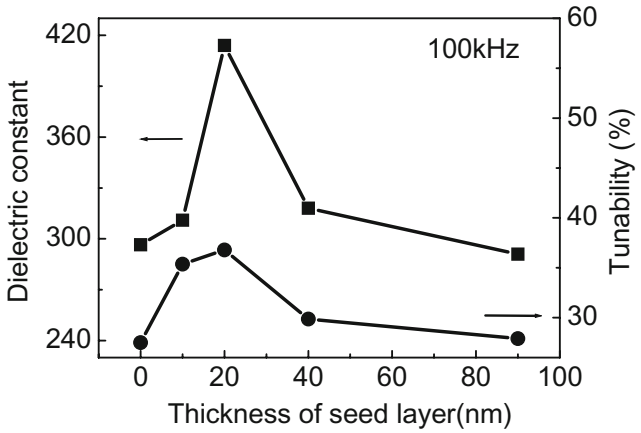

Fig. 4 Room temperature dielectric constant and tunability of BZT thin films as a function of seed layer thickness at the measurement frequency of 100 kHz

Figure 5 shows the leakage current-electric field characteristics of BZT thin films at room temperature. It can be found the current decreased to a minimum of 8.7×10^{-8} A/cm^2 with increasing in seed layer thickness to 20 nm at applied electric field of 250 kV/cm for BZT thin films. Then current increased with a further increasing in seed layer thickness above 20 nm. This behavior is due to that the microstructure BZT thin film with 20 nm seed layer in thickness was densest and smoothest in all thin films (showed in Fig. 2) and BZT thin films deposited on seed layers below a 20-nm thickness was mainly influenced by Pt bottom electrode and the BZT bulk characteristics appeared and increased while above 20-nm thickness. The leakage current characteristics are distinctly different in positive and negative electric field regions. It can be seen from Fig. 5 that the reverse currents at negative bias regions are much different from forward currents at positive bias regions. The different reverse currents might be caused by generation of a different amount of oxygen vacancy at top Au/BZT interface and at the bottom Pt/BZT interface [18].

4 Conclusions

The BZT thin films were prepared by sol–gel technique. The XRD patterns reveal that the samples are polycrystalline and single phase. FESEM analyses show that BZT thin film with 20-nm thickness seed layer reached a maximum in average grain size and became densest and smoothest in these thin

films. The dielectric constant and tunability showed a maximum of 414 and 36.8%, respectively, at a seed layer thicknesses of 20 nm, and its leakage current also reached a minimum of 8.7×10^{-8} A/cm^2 at applied electric field of 250 kV/cm. These results indicated that the optimized seed layer thickness for BZT thin films plays an important role in maintaining the high tunability and low leakage current, which are suitable for microwave device applications.

Acknowledgements This research was supported by the Ministry of Sciences and Technology of China through 973-project under grant 2002CB613304, Shanghai Nano Fundamental Committee under Contract no. 05nm05028, Special Research Fund for the Doctoral Program of Higher Education (SRFDP20060247003) and Program for New Century Excellent Talents in University (NCET).

References

1. D. Hennings, A. Schnell, G. Simon, J. Am. Ceram. Soc. **65**, 539 (1982)
2. S. Hoffmann, R.W. Waser, Integr. Ferroelectr. **17**, 141 (1997)
3. P.W. Rehrig, S.E. Park, S. Trolier-MsKinstry, G.L. Messing, B. Jones, T.R. Shrout, J. Appl. Phys. **86**, 1657 (1999)
4. Zhai Jiwei, Haydn Chen, Appl. Phys. Lett. **84**, 1162 (2004)
5. Y. Zhi, A. Chen, R. Guo, A.S. Bhalla, J. Appl. Phys. **92**, 2655 (2002)
6. S.M. Mukhopadhayay, T.C.S. Chen, J. Mater. Res. **10**, 1502 (1995)
7. J. Zhai, X. Yao, L. Zhang, B. Shen, Appl. Phys. Lett. **84**, 3136 (2004)
8. S. Hoffmann, R. Waser, J. Eur. Ceram. Soc. **19**, 1339 (1999)
9. A. Dixit, S.B. Majumder, A. Savvinov, R.S. Katiyar, R. Guo, A.S. Bhalla, Mater. Lett. **56**, 933 (2002)
10. J. Zhai, X. Yao, L. Zhang, B. Shen, H. Chen, J. Cryst. Growth **262**, 345 (2004)
11. Y.-A. Jeon, W.-C. Shin, T.-S. Seo, S.-G. Yoon, J. Mater. Res. **17**, 2831 (2002)
12. S.T. Lee, N. Fujimura, T. Ito, Jpn. J. Appl. Phys. Part 1 **34**, 5168 (1995)
13. A. Dixit, S.B. Majumder, P.S. Dobaal, R.S. Katiyar, A.S. Bhalla, Thin Solid Films **447**, 284 (2004)
14. A. Mansingh, M. Sayer, in *Proceedings of the Ninth IEEE International Symposium on Applications of Ferroelectrics (ISAF '94)*, (University Park, PA, USA, 1995), p. 663
15. A. Outzourhit, J.U. Trefny, T. Kito, B. Yarar, A. Nazirpour, A. Hermann, Thin Solid Films **259**, 218 (1995)
16. X.G. Tang, J. Wang, X.X. Wang, H.L.W. Chan, Solid State Commun. **131**, 163 (2004)
17. J.-K. Lee, Y.H. Lee, K.S. Hong, J. Appl. Phys. **95**, 219 (2004)
18. S. Maruno, T. Kuroiwa, N. Mikami, K. Sato, Appl. Phys. Lett. **73**, 954 (1998)